ASTFE
American Society
of Thermal and Fluids Engineers

8th Thermal and Fluids Engineering Conference (TFEC)
May, 2023
Partially Online Virtual and at University of Maryland, MD

TFEC-2023-45944

ANALYSIS OF IMPINGEMENT JET HEATING AND COOLING OF THERMOMAGNETIC MATERIAL

Giovanni Esposito,[1] Jonathan Hey,[2,*] & Matteo Fasano[1]

[1]Department of Energy, Politecnico di Torino, Corso Duca degli Abruzzi, 24, 10129 Torino, Italy.
[2]Agency for Science Technology and Research (A*STAR), Singapore Institute of Manufacturing Technology (SIMTech), 2 Fusionopolis Way, Singapore 138634

ABSTRACT

In this paper, an experimental study is carried out to investigate the temperature response of a thermomagnetic material subjected to water and air jet impingement. In particular, the thermomagnetic material is included in a heat energy harvesting device that uses water to heat and air to cool. The aim of the study is to enhance heat transfer and identify the limits of jet impingement to control the temperature-dependent magnetic properties of thermomagnetic materials. Beyond the Curie temperature, in fact, the material loses its magnetic properties and becomes paramagnetic. The rapid change in magnetization around the Curie temperature can be used to design a device that converts thermal energy into other useful forms of energy. The study aims to identify the suitable conditions required to operate the device and optimize the time required for heating and cooling of the material. For this reason, time dependent simulations are performed to understand how the temperature on the material varies over time for different values of water temperature and inlet velocity. Moreover, an analysis on the effect of jet impingement exit velocity, nozzle diameter and nozzle-to-surface distance on the heat transfer characteristics is made, showing the variation of the thermal time constant with these parameters.

KEY WORDS: impingement jet, energy harvesting, thermomagnetic motor

1. INTRODUCTION

Low grade heat is a byproduct of many man-made and natural processes. Recently, there has been advancement in the development of new devices and materials that can harness such low grade heat [1]. Thermomagnetic materials exhibit significant changes in magnetization following a small change in temperature around its Curie temperature. This physical property of the material can be harnessed in a device to convert thermal energy into other useful forms of energy like mechanical work [2][3][4]. A thermomagnetic motor typically consists of a movable part which is constructed from thermomagnetic material while the permanent magnetic assembly remains stationary or vice versa [5]. Typically, heat is introduced to a portion of the thermomagnetic material while the other portion is kept cool. This causes a difference in permeability between hot and cool zone which produces a net force on the material.

Rotary thermomagnetic motors produce a continuous output which makes it attractive for energy harvesting applications [6][7]. In such devices, heat is typically introduced to the thermomagnetic material through a heat transfer medium. Water is an effective medium for transferring heat energy and convenient source of low temperature heat energy [8][9]. Currently, the output of such a thermomagnetic motor is still relatively low due to the limits of heat transfer at higher rotation speed [10]. Also, not all the heat from the source can be fully utilized due to the limits of heat transfer at lower temperature while other parasitic heat losses tends to

*Corresponding Jonathan Hey: jonathan-hey@simtech.a-star.edu.sg

dominate when operating at higher temperatures [11]. Therefore, there is a need to further improve the heat transfer between the fluid medium and thermomagnetic material. Impingement jets are known to be effective ways of enhancing the local heat transfer at or near the impingement zone [12]. The localized heat transfer at the stagnation point is dependent on the exit velocity of the fluid at the nozzle and the distance of the nozzle from the solid surface as well as the diameter of the nozzle [13][14][15]. The choice of the fluid, e.g. water or air, also has a significant effect on the limits of impingement jet heat transfer [16].

In this paper, an experimental evaluation is carried out to investigate the temperature response of the thermomagnetic material in a rotary thermomagnetic motor which is subjected to water and air jet impingement. The aim of the study is to enhance heat transfer and identify the limits of jet impingement to control the temperature of the thermomagnetic materials. The suitable conditions required to operate the device and to reduce the time for heating and cooling of the material are determined from this experimental study.

2. EXPERIMENTAL EVALUATION

2.1 The thermomagnetic motor

The rotary thermomagnetic motor consists of 3 main parts: (i) outer housing, (ii) rotor and (iii) stator. Figure 1 shows a representation of the device together with the complete laboratory set-up. The rotor and stator are placed inside the outer housing which sits on bearings supported by the front and rear end caps. This creates a fully enclosed chamber which helps to contain the fluids within the device. The thermomagnetic material is located on the rotor which consists of 6 thermomagnet segments while the stator contains the permanent magnets which are positioned at a distance of approximately 10 mm from the rotor surface.

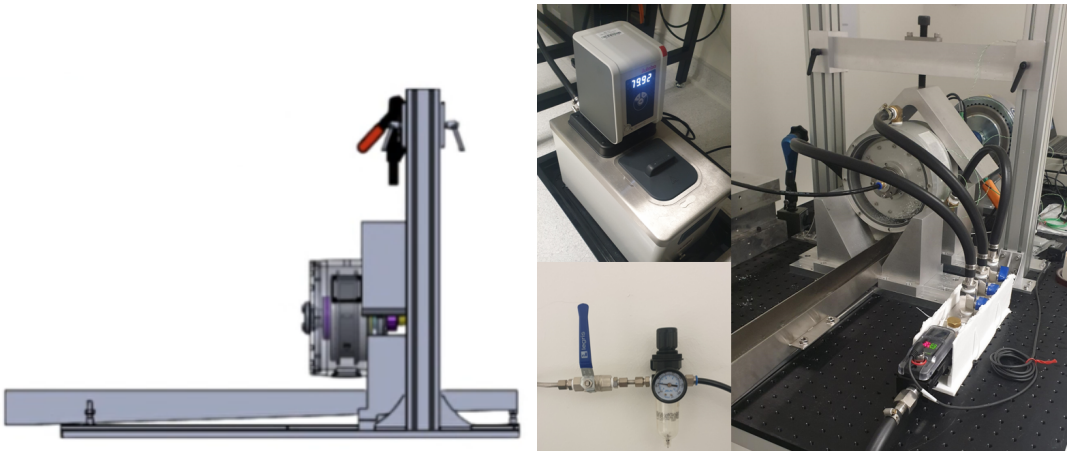

Fig. 1 The thermomagnetic motor experimental set-up.

Heat is supplied to the rotor through hot water delivered via a set of 3 nozzles positioned at 90°, 210° and 330° on the outer surface of the housing while the hot water discharge port is located at the 270° position. The hot water is maintained at 80ºC using an external heater while the flow is regulated with the built-in pump which is able to supply up to 10 L/min of hot water continuously. On the other hand, cool air is supplied to the device through a main air inlet port located on one side of the central shaft of the device. Once the cool air enters the main inlet port, it divides into 3 channels which direct the air to the inner surface of the rotor ending its run at the outlet port located on the opposite side of the device. In this case, cool air is supplied by a pressurized air source and it is regulated by means of an electronically controlled pressure valve. The heating and cooling processes are further illustrated in Figure 2. During the heating phase, hot water is supplied through the inlet at the top of the device, transferring heat to the thermomagnetic material. The temperature of the material is measured on the inner surface of the rotor as indicated in Figure 2. Once the material reaches the desired temperature or its Curie temperature, the flow of hot water is stopped and the cooling phase begins. Air at

the room temperature of about 20°C is supplied to the device. In this case, the temperature of the material is measured on the outer surface of the rotor.

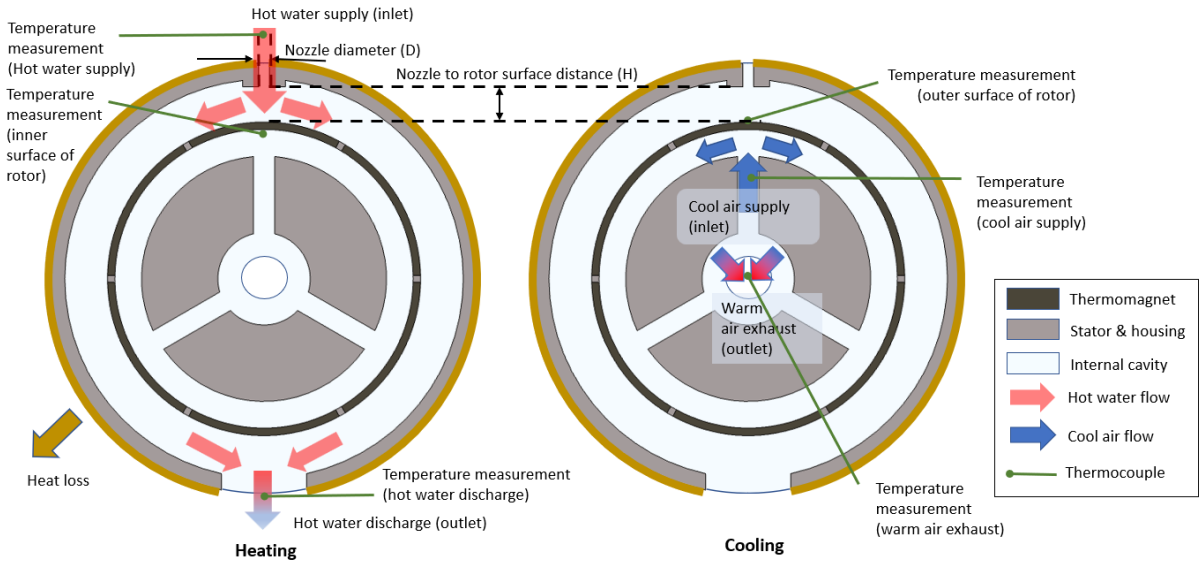

Fig. 2 Illustration of the hot water and air impingement jet.

2.2 Experimental set-up & procedure

In order to evaluate the distribution of temperature in the device, thermocouple sensors are placed in the areas of greatest interest. In fact, a sensor has been positioned on each segment of thermomagnetic material, both in the outer and inner rotor surface, as shown in the Figure 3. Furthermore, two sensors are positioned near the water inlet and outlet ports, to evaluate the supply and return hot water temperature. A sensor is placed in the air exhaust port to determine the temperature of outlet warm air. Finally, two heat flux sensors (HFS-4) are positioned on the external surface of the outer housing to determine the amount of the heat loss at the outer housing. In the subsequent thermal analysis, the inner rotor surface temperature is considered when the hot water jet is supplied while the outer rotor surface temperature is considered when the cold air jet is active. The sensor data is recorded onto a PC using Labview program for further processing thereafter. The rotor is locked in position during the experiment and only the top water inlet is used to supply the hot water. In this way, the water jet impingement is directed to outer surface of the top segment of the rotor assembly. During the cooling phase, the air pressure is varied in order to achieve different air flow rates. The measurement data is subsequently processed to evaluate the heat transferred to and from the fluid during both phases under the various conditions tested. Each experiment is characterized by the following 3 phases: (i) pre-heating, (ii) cooling and (iii) heating which would be further illustrated in the results section. A series of experiments is conducted by varying the following parameters: (i) nozzle diameter (D), (ii) nozzle to rotor surface distance (H) and (iii) water and air flow rates ($\dot{V}$). The following table shows the range of values for each of the parameters considered in this analysis

Parameters	Range of values
Water flow rate ($\dot{V}$)	1 to 5 L/min
Nozzle diameter (D)	4 or 5 mm
Nozzle to rotor surface distance (H)	14 or 20 mm
Air Pressure	0.3 to 1.5 bar

Table 1 List of parameters and the range of values considered.

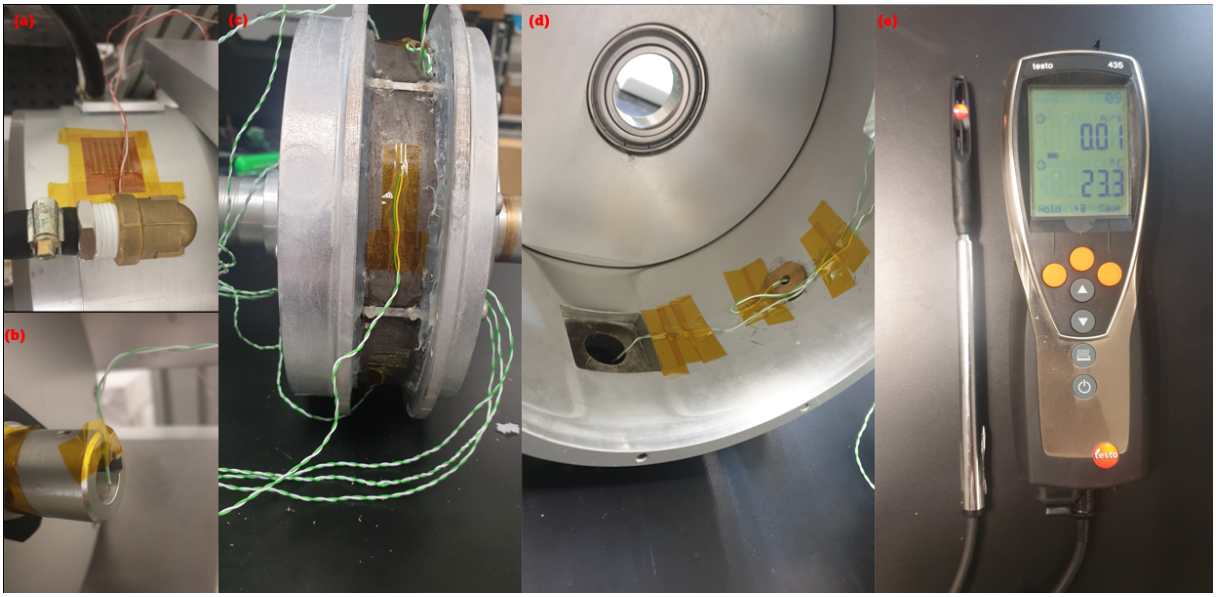

Fig. 3 (a) Heat Flux Sensor (HFS-4), (b) air outlet temperature sensor, (c) rotor surface temperature sensors, (d) water inlet and outlet temperature sensors, (e) air velocity sensor.

2.3 Thermal analysis

In this section, the evaluation of the heat flux and the related thermal transmittance is described and elaborated. The rate of heat transferred from the water during heating is given by the following formulation:

$$\dot{Q}_{heat} = \rho_w C_w \dot{V}_w (T_{w,out} - T_{w,in}) + \dot{Q}_{loss} \tag{1}$$

where $T_{w,out}$ is the temperature of water at the outlet, $\dot{V}_w$ is the volume flow rate of water while ρ_w is the density and C_w is the specific heat capacity of water. Moreover, $\dot{Q}_{loss}$ represents the total thermal power loss during the experiment. During the heating process, the specific heat flux ($\dot{Q}''_{heat}$) on the exposed area (A) of the rotor is given by the following expression:

$$\dot{Q}''_{heat} = \frac{\dot{Q}_{heat}}{A} \tag{2}$$

Thereafter, the average thermal transmittance can be evaluated as:

$$U_{heat} = \frac{\dot{Q}''_{heat}}{(T - T_{w,in})} \tag{3}$$

whereby T is the average temperature of the thermomagnetic material and $T_{w,in}$ is the temperature of the hot water at the inlet, which is maintained at 80 °C. For the specific heat capacity, the value considered for water is $C_w = 4190$ J/Kg-K while the density of water is a function of temperature, $\rho_w(T)$.

During the cooling process, the rate of heat transferred to the air is evaluated as follow:

$$\dot{Q}_{cool} = \rho_a C_a \dot{V}_a (T_{a,out} - T_{a,in}) + \dot{Q}_{loss} \tag{4}$$

where $T_{a,out}$ is the average value of the air temperature at the outlet while the inlet air $T_{a,in}$ is fixed to be at 20 °C. The specific heat capacity of air is assumed to be constant at $C_a = 1007$ J/Kg-K while the density of air is taken as a function of its temperature and pressure $\rho_a(P, T)$. The specific heat flux ($\dot{Q}''_{cool}$) on the rotor

surface during cooling is then evaluated with the following expression:

$$\dot{Q}''_{cool} = \frac{\dot{Q}_{cool}}{A} \tag{5}$$

and the thermal transmittance during cooling is evaluated as:

$$U_{cool} = \frac{\dot{Q}''_{cool}}{(T - T_{a,in})} \tag{6}$$

An example of the measurement data obtained from the experiments is shown in Figure 4. It shows the span of the data that are used in the evaluation of the heat transfer parameters that will be presented in the next section. The different colored lines represents temperature measurements obtained from the inner and outer surface of the rotor.

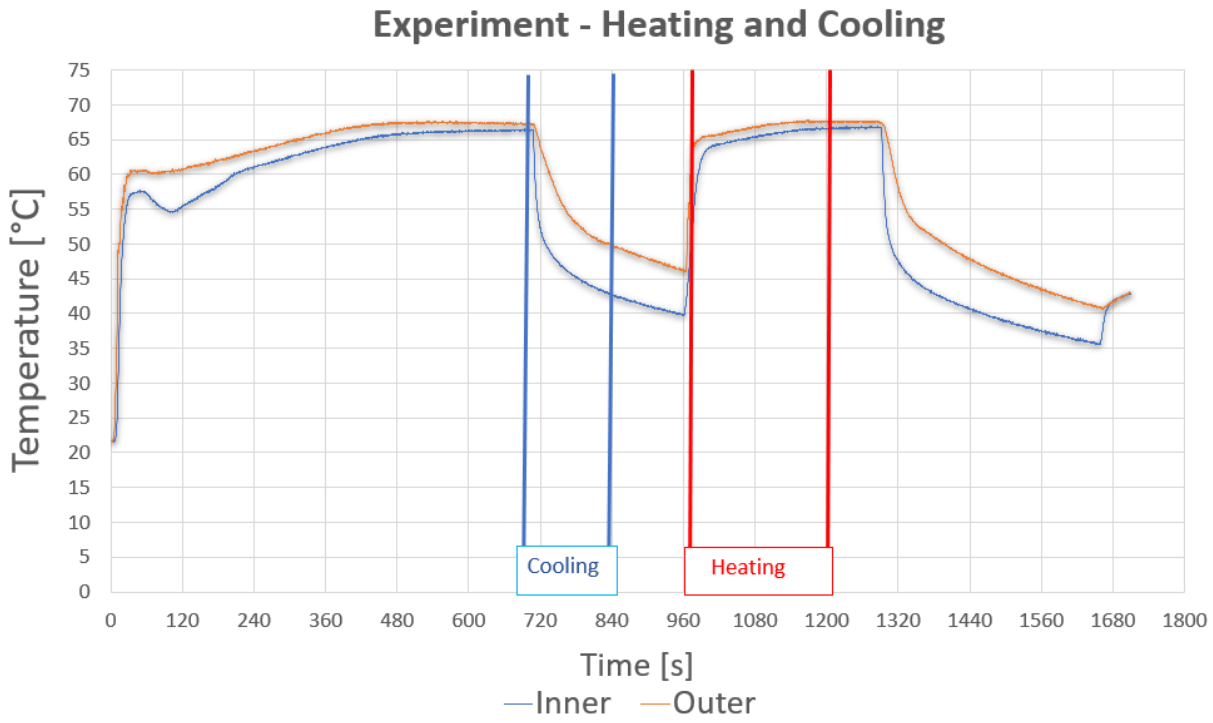

Fig. 4 Laboratory experiments - Data record through Labview.

3. EXPERIMENTAL RESULTS

Figure 5 shows the heat flux and thermal transmittance achieved during the heating phase. It is clear that, during the heating phase, the 4 mm diameter nozzle yields greater heat transfer. A maximum value of specific heat flux of $\dot{Q}''$ = 104 kW/m^2 is achieved with the 4 mm nozzle at a separation distance of 20 mm. Reducing the separation distance does not yield a better heat transfer. In fact, the heat flux achieved with this configuration does not exceed the prior configuration at all. Even though the fluid jet does not reach the higher velocities with the 5 & 6 mm diameter nozzles, the downward trend of the heat flux after a fluid velocity of 2.5 m/s shows that the heat transfer is not likely to increase any further beyond that point. The result clearly shows that the 4 mm diameter nozzle out performs the 5 & 6 mm nozzles especially at higher velocities. This shows the strong dependency of the heat transfer with the fluid jet velocity. The thermal transmittance provides an

additional dimension to the analysis since it also accounts for the rise in the temperature of the material. It provides an indication of the effectiveness of the impingement jet in heating up the thermomagnetic material. A maximum U = 7400 W/m^2-K is achievable with the same configuration where the peak flux occurs.

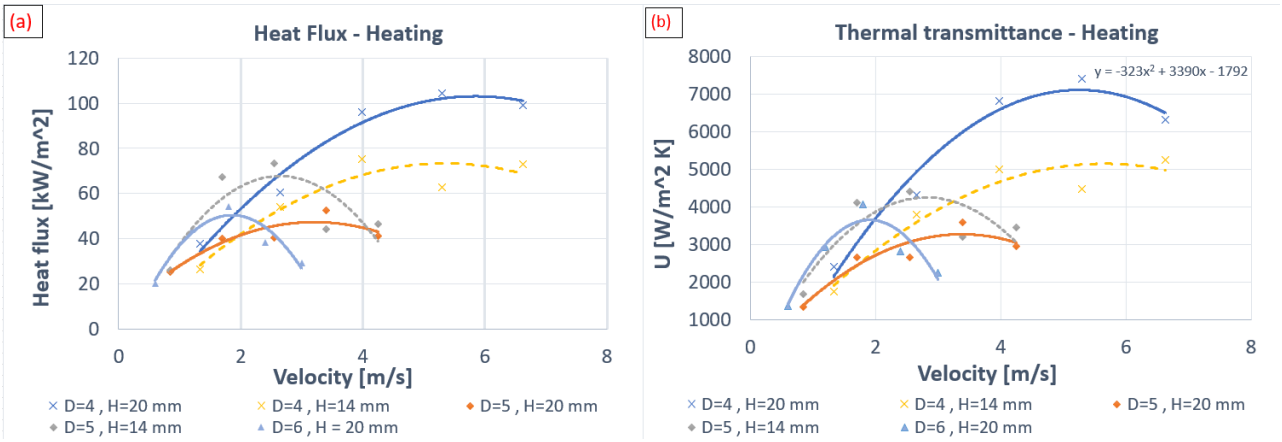

Fig. 5 (a) Heat flux and (b) Thermal transmittance derived during heating by water jet.

Figure 6 shows the heat flux and thermal transmittance achieved during the cooling phase. The inlet velocity of the air jet is varied by regulating the supply of air between 0.3 to 1.5 bar. The corresponding velocity of the air jet is determined to be between 4 m/s to 8.5 m/s. A maximum specific heat flux of $\dot{Q}''$ = 8 kW/m^2 and a corresponding thermal transmittance of U = 265 $\mathrm{W/m^2}$-K is achieved at the maximum air velocity of 8.5 m/s. The rate of heat transfer is still significantly lower than that achieved during the heating phase. This is mainly due to air being used as the medium for heat transfer during the cooling phase. The lower thermal capacity and diffusivity of air do present a limit to achieving rapid cooling of the thermomagnetic material. Increasing the inlet air velocity is expected to further increase the heat transfer as indicated by the upward sloping trendline in Figure 6. Cooling of the material does represents a real limitation to the operation of the device especially if higher rotation speed is to be achieved.

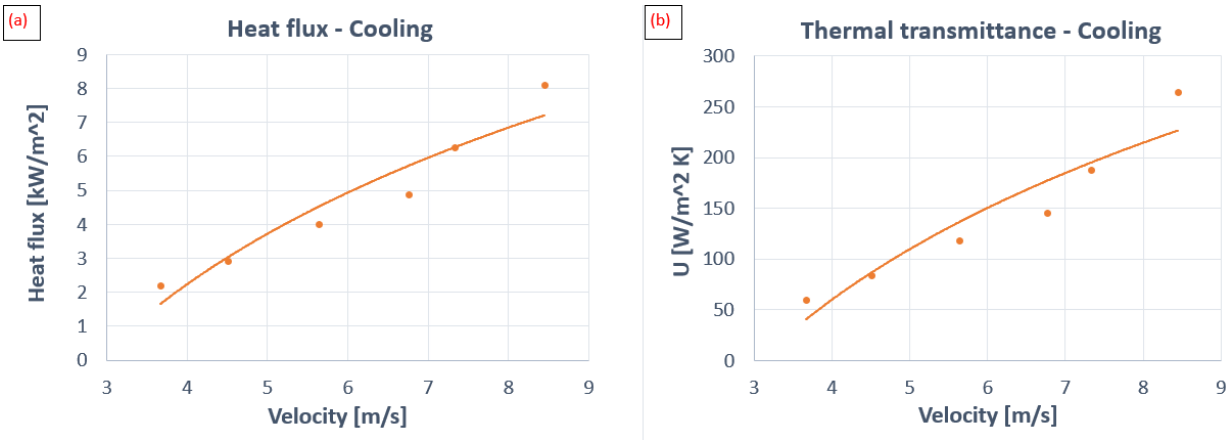

Fig. 6 (a) Heat flux and (b) Thermal transmittance derived during cooling by air jet.

Figure 7 shows the temperature response on the thermomagnetic material under the more ideal conditions as identified from the experimental testing. It is evident that the temperature of the material responds more rapidly to using the 4 mm nozzle at 20 mm separation distance compared to other the configurations evaluated. The material is able to reach its Curie temperature of about 60°C in less than 7s which represents a reduction of more than 5s from the other configuration shown in Figure 7. On the other hand, cooling down the material to the Curie temperature takes more than 17s with the highest air velocity. This still represents a significant delay when compared to the heating process. The asymmetric heating and cooling of the material would lead

to some challenges in the operation of the device.

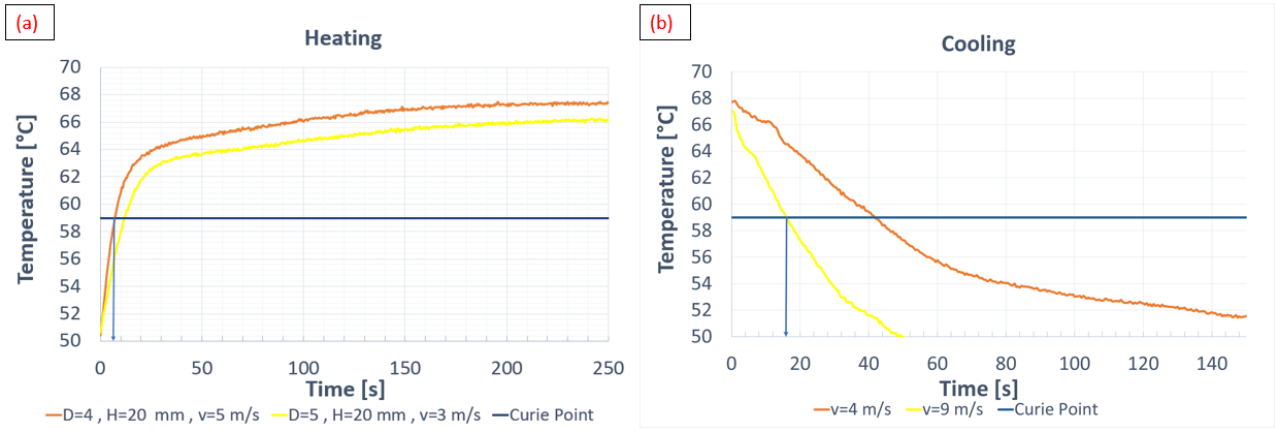

Fig. 7 (a) Heating and (b) cooling curve under the ideal operating conditions.

4. CONCLUSION

In this paper, an experimental investigation is carried out to analyse the heat transfer characteristics of an impinging fluid jet directed onto the curved surface of the rotor of a thermomagnetic motor. Hot water is used as the heat source during the heating phase while cold air is chosen as the medium during the cooling phase. The heat flux and thermal transmittance during both the heating and cooling phases are evaluated from the data obtained from the experiments. A series of tests is conducted with nozzles of different diameters and nozzle-to-surface distance, as well as various inlet velocity of the hot water to determine the conditions necessary to maximize heat transfer. During the heating phase, it is observed that a nozzle diameter of 4 mm and a separation distance of 20 mm is the configuration that performs best. A heat flux of $\dot{Q}'' = 104\,\mathrm{kW/m^2}$ and thermal transmittance of $U = 7400\,\mathrm{W/m^2{-}K}$ is achieved with an inlet velocity of about 5 m/s. In general, the nozzle with the smaller diameter out performs the larger diameter nozzles due to the higher inlet velocity attained. As for the cooling phase, the highest rate of heat transferred is reached with a maximum air velocity of 8.5 m/s. In this case, a heat flux of $\dot{Q}'' = 8\,\mathrm{kW/m^2}$ and thermal transmittance of $U = 265\,\mathrm{W/m^2{-}K}$ is achieved. In both cases, the results show that the rate of heat transferred to and from the fluid jet during cooling and heating has a strong dependency on the inlet velocity of the fluid and the choice of fluid. The lower capacity of air to store and transfer heat does pose a limit to achieving higher rates of heat transfer during cooling. At the optimal operating conditions, the time taken for the thermomagnetic material to reach its Curie temperature for heating is about 7s while it takes about 17s during the cooling phase. This represents a 5-15s reduction in the heating and cooling time required during the operation of the thermomagnetic motor respect to previous operating conditions, which would allow to reach to a higher rotation speed and also increased output power from the thermomagnetic motor.

ACKNOWLEDGEMENT

The authors would like to acknowledge the support of the Agency for Science, Technology and Research (A*STAR) through the Career Development Award (202D800030) which has provide the necessary resource for the authors to carry out the research activities that led to this publication.

References:

[1] R. A. Kishore and S. Priya, "A review on design and performance of thermomagnetic devices," Renew. Sustain. Energy Rev., vol. 81, pp. 33–44, 2018, doi: https://doi.org/10.1016/j.rser.2017.07.035.

[2] D. Zabek and F. Morini, "Solid state generators and energy harvesters for waste heat recovery and thermal energy harvesting," Therm. Sci. Eng. Prog., vol. 9, no. November 2018, pp. 235–247, 2019, doi: 10.1016/j.tsep.2018.11.011.

[3] Zeeshan, M. U. Mehmood, and S. Cho, "Optimization of a thermomagnetic heat engine for harvesting low grade thermal energy," Energies, vol. 14, no. 18, pp. 1–16, 2021, doi: 10.3390/en14185768.

[4] M. Trapanese, G. Cipriani, V. Di Dio, V. Franzitta, and A. Viola, "Optimization of a thermomagnetic motor," J. Appl. Phys., vol. 117, no. 17, 2015, doi: 10.1063/1.4919231.

[5] J. Hey, T. Jun Liang, and T. Zhi Hao, "An evaluation of thermomagnetic motors for heat energy harvesting," in 2022 IEEE/ASME International Conference on Advanced Intelligent Mechatronics (AIM), 2022, pp. 1347–1354, doi: https://doi.org/10.1109/AIM52237.2022.9863263.

[6] Y. Takahashi, T. Matsuzawa, and M. Nishikawa, "Fundamental performance of the disc-type thermomagnetic engir," Electr. Eng. Japan (English Transl. Denki Gakkai Ronbunshi), vol. 148, no. 4, pp. 26–33, 2004, doi: 10.1002/eej.10359.

[7] J. Hey, M. Repaka, T. Li, and J. L. Tan, "Design Optimization of a Rotary Thermomagnetic Motor for More Efficient Heat Energy Harvesting," Energies, vol. 15, no. 6334, 2022, doi: https://www.mdpi.com/1996-1073/15/17/6334.

[8] G. P. Hammond and J. B. Norman, "Heat recovery opportunities in UK industry," Appl. Energy, vol. 116, pp. 387–397, Mar. 2014, doi: 10.1016/j.apenergy.2013.11.008.

[9] C. S. Alves, F. C. Colman, G. L. Foleiss, W. Szpak, T. F. Vieira, and A. C. Bento, "Simulation of solar Curie wheel using NiFe alloy and Gd," Int. J. Refrig., vol. 37, no. 1, pp. 215–222, 2014, doi: 10.1016/j.ijrefrig.2013.09.031.

[10] K. Deepak, M. S. Pattanaik, and R. V. Ramanujan, "Figure of merit and improved performance of a hybrid thermomagnetic oscillator," Appl. Energy, vol. 256, no. May, p. 113917, 2019, doi: 10.1016/j.apenergy.2019.113917.

[11] Zeeshan et al., "Operation of a low-temperature differential heat engine for power generation via hybrid nanogenerators," Appl. Energy, vol. 285, no. June 2020, p. 116385, 2021, doi: 10.1016/j.apenergy.2020.116385.

[12] K. Jambunathan, E. Lai, M. A. Moss, and B. L. Button, "A review of heat transfer data for single circular jet impingement," Int. J. Heat Fluid Flow, vol. 13, no. 2, pp. 106–115, 1992, doi: 10.1016/0142-727X(92)90017-4.

[13] I. Mudawar, "Assessment of high-heat-flux thermal management schemes," IEEE Trans. Components Packag. Technol., vol. 24, no. 2, pp. 122–141, Jun. 2001, doi: 10.1109/6144.926375.

[14] E. M. Dede, "Multiphysics optimization, synthesis, and application of jet impingement target surfaces," pp. 1–7, 2010.

[15] Guoxin, hu & Zhang, Lixiang. (2007). Experimental and Numerical Study on Heat Transfer with Impinging Circular Jet on a Convex Hemispherical Surface. Heat Transfer Engineering - HEAT TRANSFER ENG. 28. 1008-1016. 10.1080/01457630701483638.

[16] A. V. S. Oliveira et al., "Experimental study of the heat transfer of single-jet impingement cooling onto a large heated plate near industrial conditions," Int. J. Heat Mass Transf., vol. 184, p. 121998, 2022, doi: 10.1016/j.ijheatmasstransfer.2021.121998.